Microstructure observations on butt joint composed of Nb3Sn CIC conductors

Microstructure observations on butt joint composed of Nb_3Sn CIC conductors

Tetsuhiro Obana[a]*, Masayuki Tokitani[a], Kazuya Takahata[a], Kaname Kizu[b], Haruyuki Murakami[b]

National Institute for Fusion Science, National Institutes of Natural Sciences[a], 322-6 Oroshi, Toki, Gifu, 509-5292, Japan
National Institutes for Quantum and Radiological Science and Technology[b], 801-1 Mukoyama, Naka, Ibaraki, 311-0193, Japan

*Corresponding author. Tel.: +81 572 58 2137 ; fax: +81 572 58 2616
E-mail address: obana.tetsuhiro@LHD.nifs.ac.jp (T. Obana)

Abstract

To precisely evaluate a butt joint technology for the JT-60SA CS coils, microstructure observations on the butt joint composed of Nb_3Sn CIC conductors were conducted using a FE-SEM. As a sample for the observations, the butt joint sample utilized in the joint resistance measurement was used. During the sample fabrication, the butt joint sample was heated up to about 920 K from room temperature for diffusion bonding after heat treatment for Nb_3Sn production. Then, the sample was subjected to the cycles of electromagnetic force in the joint measurement.

The observation results indicated that Nb_3Sn strands and a copper sheet were butted properly at the interface of the butt joint. In addition, there were hairline cracks in the Nb_3Sn layers of the strands near the interface. To investigate a cause of the crack initiation, the stresses generated in the butt joint under same conditions were analyzed using a simple model. As a result, the cracks would occur with an axial compressive stress generated by the butt joint fabrication.

Keywords:
Butt joint
Cable-in-conduit (CIC) conductor
JT-60SA central solenoid (CS)
Nb_3Sn
Microstructure observation

1. Introduction

In the JT-60 Super Advanced (JT-60SA) fusion experiment, the magnet system consists of a central solenoid (CS) coil, 18 toroidal field coils, and six plasma equilibrium field (EF) coils [1-3]. The CS coil is composed of four modules. One module is composed of six octa-pancake coils and four quad-pancake coils. To join these coils, wound with Nb_3Sn cable-in-conduit (CIC) conductors, a butt joint technology was adopted in the CS coil. The butt joint is very attractive choice for the CS coil of a Tokamak machine because it allows embedding of the joint into a winding pack that provides maximum flux at a given peak field in the winding [1]. To evaluate the fabrication technology of the butt joint, a joint resistance was measured using a butt joint sample. As a result, the sample fulfilled the design requirement of joint resistance [4-6].

Compared to a lap joint technology, the butt joint technology is emerging and challenging at present. Hence,

not only joint resistance but also microstructural observation is necessary to fully evaluate the butt joint. In this study, a joint interface of the butt joint sample was observed using a field emission scanning electron microscope (FE-SEM) after the joint measurements.

2. Joint resistance measurements of the butt joint sample

2-1. Butt joint sample

As illustrated in Fig. 1, the butt joint sample is hairpin-shaped and consists of two butt joints using the JT-60SA CS conductors [5,6]. The CS conductor is a CIC conductor composed of Nb_3Sn strands and copper wires. The cross-sections of the conductor, Nb_3Sn strand, and filaments are shown in Fig. 2. Details of the conductor are listed in Table 1. The butt joint sample has a single inlet and double outlets for supercritical helium (SHe). At the termination, Nb_3Sn cables are connected to an oxygen-free copper plate by sinter bonding.

Fig. 3 shows the photograph and configuration of the butt joint without a conduit. The cross-section of the butt joint with the conduit is illustrated in Fig. 4. In terms of butt joint fabrication, the conduit is removed to expose the Nb_3Sn cable before heat treatment of the Nb_3Sn strands. The central spiral is replaced with a cone-shaped flow distributor. The cables are compacted to 2% void fraction using copper sleeves. Joining surfaces of the cables are cut and polished after the heat treatment. A 0.1-mm-thick copper sheet is then inserted in between the butted surfaces. The joining part is heated for diffusion bonding in a vacuum. The conduit and spacers are then assembled. Details of the butt joint fabrication are described in Ref. [4].

2-2. Measurement results of joint resistance

Joint resistances of the butt joint sample were measured under several conditions using the NIFS test facility [7]. The measurement results are listed in Table 2. The measurements (Experimental run number: CSB04 - CSB07) were conducted at 4.5 K before the quench tests of the butt joint (Experimental run number: CSB09 - CSB32). After the quench tests, the measurements (Experimental run number: CSB33) was conducted at 7 K. Details of the experimental run number are described in Fig.5

The results indicated that the performance of the butt joint fulfilled the design requirement in which the joint resistance was less than 5 nΩ under 2 T [4-6].

2-3. EM force and temperature histories of the butt joint sample

Fig. 5 shows the electromagnetic(EM) forces loaded to the butt joint sample during the measurement. In the real-world operation of the CS coils, the EM force is 40 kN/m at a maximum. Hence, the sample was subjected to overload conditions.

Temperature history of the butt joint sample was summarized in Fig. 6. The sample was heated twice up to about 920 K from room temperature during the sample fabrication. Subsequently, the sample was cooled down to about 4 K.

3. Microstructural observations of the butt joint interface

3-1. Sample for the microstructural observations

To make a sample for the microstructural observations, vacuum impregnation of the butt joint sample was conducted after the joint measurement, and the butt joint sample was sundered around the butt joint interface. Then, a piece sundered from the butt joint sample was split. Finally, surfaces split from the piece were polished for the

observation using a FE-SEM. The process of the sample fabrication is summarized in Fig. 7. In terms of the surface polishing, four processes were conducted with several materials and tools listed in Table 3.

3-2. Observations

Microstructural observations of a butt joint interface were conducted using the FE-SEM (Model number: JSM-7100F, JEOL Ltd.) . Fig. 8 shows the micrographs of the butt joint interface at a strand scale. The configurations of Nb_3Sn strands, copper wires and a copper sheet were clearly observed in Fig. 8. These micrographs indicated that Nb_3Sn strands and a copper sheet were butted properly. To investigate the condition of Nb_3Sn layers, the butt joint interface was observed at a filament scale. Fig. 9 shows the Nb_3Sn layers close to the butt joint interface. In some of Nb_3Sn layers which are brittle materials, there were hairline cracks perpendicular to the copper sheet. On the contrary, the cracks did not occur in Nb cores and Cu-Sn matrix which are ductile materials. Additionally, in Cu-Sn matrix, there were many voids the size of which were various.

4. Discussion

4-1. Differentiation between hairline crack and scratch in the sample for the microstructural observations

As described in section 3-1, a sample was polished for the microstructural observation. Although the polishing was conducted carefully not to damage the sample, scratching the sample might occur during the polishing. In terms of evaluating the condition of Nb_3Sn layers, the scratch must not be mistaken for hairline cracks. Hence, we distinguished the hairline crack from the scratch using the micrographs of the butt joint interface. As shown Fig. 9, the hairline cracks are not straight lines but curved jaggy lines. On the contrary, the scratch is straight as shown in Fig. 10. Consequently, marks made on Nb_3Sn layers are definitely cracks in Fig. 9.

4-2. The cause of crack initiation

Hairline cracks in Nb_3Sn layers propagated in the longitudinal direction of a Nb_3Sn strand as shown in Fig. 9. As a cause for the crack initiation, two events for a joint sample are considered as follows: the butt joint fabrication and energization. The stresses generated by the two events were evaluated quantitatively using a simple analytical model.

In the butt joint fabrication, a joining part was heated from room temperature to 928 K under an axial compressive stress of 30 MPa [4]. To evaluate a stress generated by the joint fabrication process, an analytical model consisting of Nb_3Sn and copper was used based on the theory of composites. The model is assumed to be a compacted cable attached to a copper sheet as illustrated in Fig. 11. The model is a one dimensional model in the axial direction of the butt joint. As for boundary conditions, the one side on the model is fixed, and the other side is free. At the other side, however, the surfaces of Nb_3Sn and copper are homologous. In the model, Young's modulus of Nb_3Sn and copper are 165 GPa and 114 GPa, respectively [8].

In the process of butting cables with the axial compressive stress, the stress generated in Nb_3Sn is given by

$$\sigma_{Nb3Sn} = \frac{E_{Nb3Sn}\cdot(A_{Nb3Sn}+A_{Cu})}{E_{Nb3Sn}\cdot A_{Nb3Sn}+E_{Cu}\cdot A_{Cu}}\sigma \qquad (1)$$

where σ is the axial compressive stress, σ_{Nb3Sn} is the stress generated in Nb_3Sn, A_{Nb3Sn} is the cross-sectional area of Nb_3Sn, A_{Cu} is the cross-sectional area of copper, E_{Nb3S} is Young's modulus of Nb_3Sn, and E_{Cu} is Young's modulus of copper. As for the ratio of cross-sectional area, A_{Cu}/A_{Nb3Sn} is 4. Using Eq.1, the stress for Nb_3Sn is a compressive stress of 39.9 MPa in the longitudinal direction of the cable.

Additionally, in this evaluation, a stress generated in Nb_3Sn is assumed to be 0 Pa when the temperature of Nb_3Sn is close to that of Nb_3Sn formation temperature (923 K). Therefore, in the case that the joint part was heated up

to 928 K from room temperature, the thermal stress generated in Nb_3Sn is 0 Pa.

In the evaluation of a stress for Nb_3Sn by the energization as described in Section 2.3, Eq.2 is utilized as written:

$$\sigma_{EM} = \frac{F_{EM}}{l} \qquad (2)$$

where F_{EM} is EM force per unit length, l is one-half of a perimeter of a cable attached to a copper sheet. Eq.2 can calculate a stress by EM force in the radial direction of a cable. Using Eq.2, the stress for Nb_3Sn was derived as a compaction stress of 3.2 MPa in a radial direction of the cable.

Through the evaluations for each event as described above, the axial compressive stress of the butt joint fabrication is dominant as a stress generated in Nb_3Sn. Provided that cracks in Nb_3Sn layer occur by the stress due to the energization, the cracks will initiate in the direction perpendicular to the tensile stress caused by the EM force, as illustrated in Fig. 12. In Ref.[9], the cracks have already been observed in bronze-processed Nb_3Sn strand subjected to an EM force using ITER conductor samples. Consequently, the compressive stress due to the butt joint fabrication will be a cause of the crack initiation along the longitudinal direction as shown in Fig. 9.

4-3. Concern about the performance degradation of the butt joint

Once a hairline crack is generated in the Nb_3Sn layer of the butt joint, it is possible that the crack will propagate and enlarge due to repeated EM cycles and thermal cycles which would be expected in real-world operations of the JT-60SA CS coils. In addition, the superconducting characteristics of the Nb_3Sn layer would be degraded by the crack, and as a result, the joint resistance will increase because of this crack. Therefore, the influence of the crack on the butt joint performance is a concern. To address this issue, it is necessary to understand how the crack propagates and enlarges in Nb_3Sn layer under the EM and thermal cycles. In terms of cost, a numerical simulation of the crack is suitable for a realistic solution.

5. Conclusion

To precisely investigate the butt joint composed of Nb_3Sn CIC conductors, microstructural observations of the butt joint were conducted using a FE-SEM. As a sample for the microstructural observation, the butt joint sample used in the joint resistance measurement was utilized by reprocessing the configuration of the joint sample. The observation results indicated that Nb_3Sn strands and a copper sheet were butted properly at the interface of the butt joint. Additionally, in the Nb_3Sn layer of the strands near the interface of the butt joint, there were hairline cracks perpendicular to the copper sheet. To identify a cause of the crack initiation, an analysis was conducted using a model assuming the butt joint configuration. As a result, the hairline cracks would occur with an axial compressive stress in the longitudinal direction of a cable during the butt joint fabrication.

Acknowledgments

The authors thank Dr. Tamura of NIFS and the staff members of Hitachi Power Solutions Co. for their technical support.

References

[1] K. Yoshida, K. Tsuchiya, K. Kizu, H. Murakami, K. Kamiya, T. Obana, et al., Development of JT-60SA superconducting magnet system, Physica C, 470 (2010) 1727-1733.

[2] K. Yoshida, H. Murakami, K. Kizu, K. Tsuchiya, K. Kamiya, Y. Koide, et al., Mass Production of Superconducting Magnet Components for JT-60SA, IEEE Transactions on Applied Superconductivity, 24(2014) 4200806.

[3] H. Murakami, K. Kizu, K. Tsuchiya, Y. Koide, K. Yoshida, T. Obana, et al., Development and Test of JT-60SA Central Solenoid Model coil, IEEE Transactions on Applied Superconductivity, 24 (3) (2014) 4200205.
[4] K. Kizu, H. Murakami, K. Tsuchiya, K. Kiyoshi, K. Nomoto, Y. Imai, et al., Development of Central Solenoid for JT-60SA, IEEE Transactions on Applied Superconductivity, Vol. 23, No. 3 (2013) 4200104.
[5] T. Obana, K. Takahata, S. Hamaguchi, K. Natsume, S. Imagawa, T. Mito, et al., Modeling of Butt Joint Composed of Nb_3Sn Cable-In-Conduit Conductors, Plasma and Fusion Research, Vol. 9 (2014) 3405122.
[6] T. Obana, K. Takahata, S. Hamaguchi, K. Kizu, H. Murakami, H. Chikaraishi, et al., Conductor and joint test results of JT-60SA CS and EF coils using the NIFS test facility, Cryogenics, Vol. 73 (2016) 25-41.
[7] T. Obana, K. Takahata, S. Hamaguch, N. Yanagi, T. Mito, S. Imagawa, et al., Upgrading the NIFS superconductor test facility for JT-60SA cable-in-conduit conductors, Fusion Engineering and Design, 84 (2009) 1442-1445.
[8] S. Murase, H. Okamoto, FEM Analysis of three directional strain states under applied tensile stress for various composite superconductors, IEEE Transactions on Applied Superconductivity, Vol. 14, No. 2 (2004) 1130-1134.
[9] C. Sanabria, P. J. Lee, W. Starch, I. Pong, A. Vostner, M. C. Jewell, et al., Evidence that filament fracture occurs in an ITER toroidal field conductor after cyclic Lorentz force loading in SULTAN, Superconductor Science and technology, Vol. 25 (2012) 075007.

Figure Captions

Fig. 1 Configuration of the butt joint sample.
Fig. 2 Cross-sections of the CIC conductor, Nb_3Sn strand, and superconducting filament.
Fig. 3 Photograph and configuration view of the butt joint without a conduit.
Fig. 4 Cross-section of the butt joint.
Fig. 5 History of electromagnetic force generated in the butt joint sample during the measurement.
Fig. 6 Temperature history of the butt joint sample.
Fig. 7 Fabrication process of the sample for microstructure observation.
Fig. 8 Microstructure observation results of the butt joint interface at a strand scale. (a) Filaments of Nb_3Sn strands are attached to the copper sheet. (b) Cu stabilizer of Nb_3Sn strands are attached to the copper sheet.
Fig. 9 Microstructure observation result of the butt joint interface at a filament scale.
Fig. 10 Microstructure observation result of scratches by polishing.
Fig. 11 Analytical model of the butt joint based on the theory of composites.
Fig. 12 Schematic view of the crack propagating in the direction perpendicular to the tensile stress

Table 1 Main parameters of CS conductor.

Nb_3Sn filament diameter [μmm]	3.5 (Nominal value)
Number of Nb_3Sn filament	8130
Strand diameter [mm]	0.82
Strand surface	Cr plating (1.6 μm)
Cu/non-Cu ratio	1.0
Number of Nb_3Sn strands	216
Number of Cu wires	108
Cabling pattern	(2 +1Cu) ×3×6×6
Twist pitch [mm]	45/85/125/160
Sub-wrapping	w/o
Void fraction [%]	34
Jacket outer size [mm×mm]	27.9×27.9
Cabling diameter [mm]	21.0
Central spiral (id/od) [mm]	7/9

Table 2 Joint resistance of the butt joint sample

Magnetic field [T]	Joint resistance [nΩ]	
	at 4.5 K	at 7.0 K
0	1.24	-
1	1.55	-
2	1.91	2.11
3	2.20	-
4	2.46	-

Table 3 Polishing Tool and material used at each process

Process	*Polishing Tool*	*Polishing material*
Ⅰ	MD-Fuga (φ300)	Sic polishing paper (#220, #500, #1000, #240)
Ⅱ	MD-Dac (φ300)	Diamond-slurry (3 μm)
Ⅲ	MD-Nap (φ300)	Diamond-slurry (1 μm)
Ⅳ	MD-Nap (φ300)	Colloidal silica

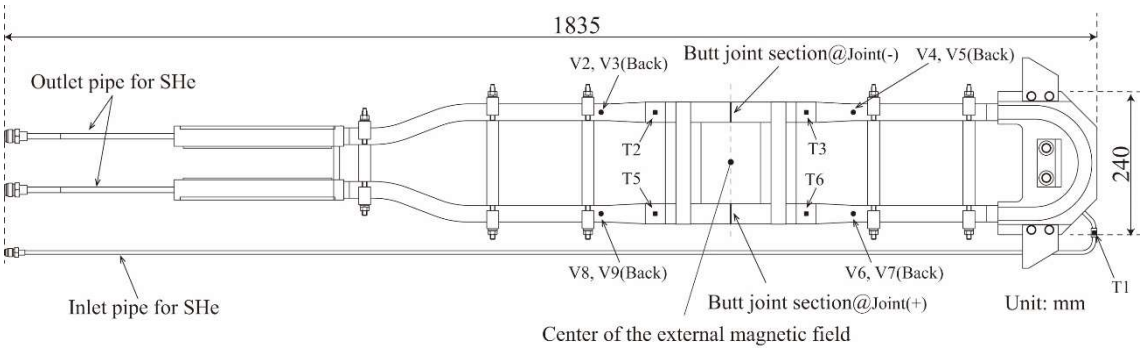

Fig. 1 Configuration of the butt joint sample.

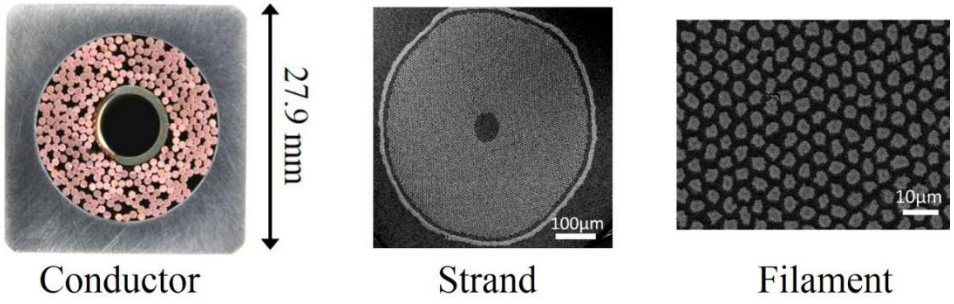

Fig. 2 Cross-sections of the CIC conductor, Nb_3Sn strand, and superconducting filaments.

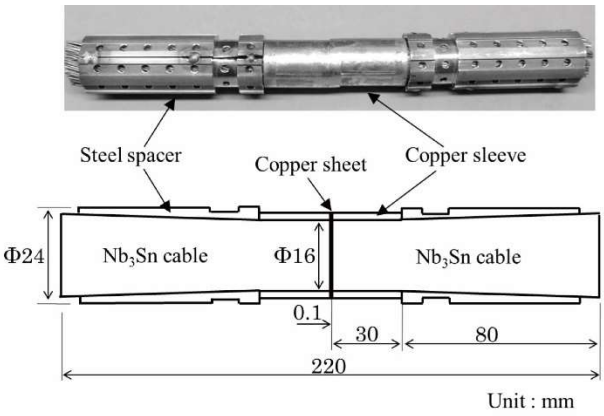

Fig. 3 Photograph and configuration view of the butt joint without a conduit.

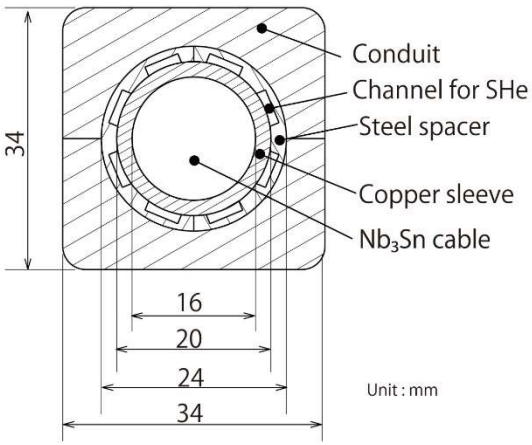

Fig. 4　Cross-section of the butt joint.

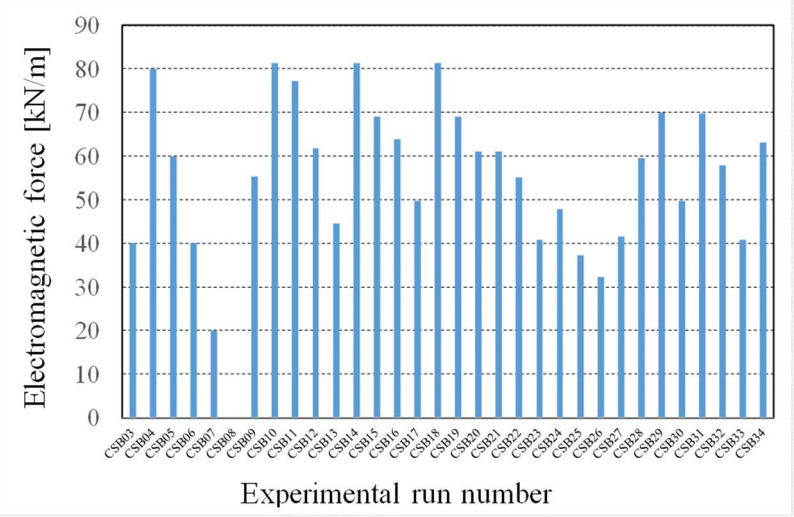

Fig. 5　History of electromagnetic force generated in the butt joint sample during the measurement.

∗ Experimental run number “CSB04~CSB07“ : Joint resistance measurement at 4.5 K.

∗ Experimental run number “CSB09~CSB32, CSB34“ : Quench test.

∗ Experimental run number “CSB33“ : Joint resistance measurement at 7 K.

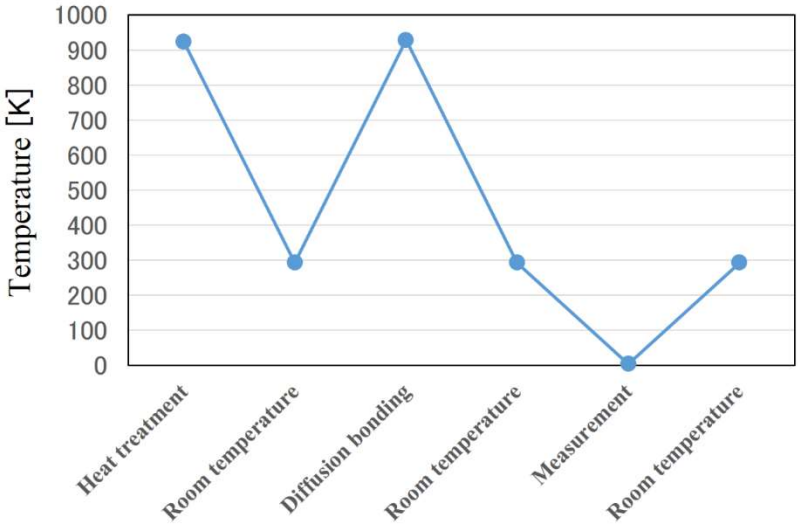

Fig. 6　Temperature history of the butt joint sample.

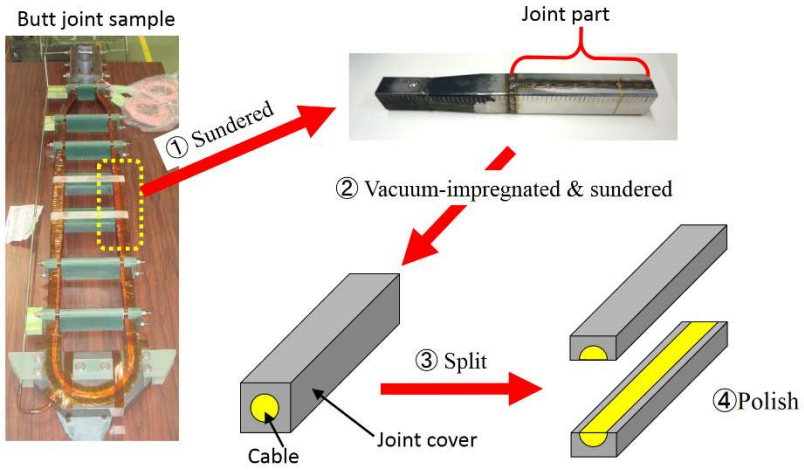

Fig. 7　Fabrication process of the sample for microstructure observation.

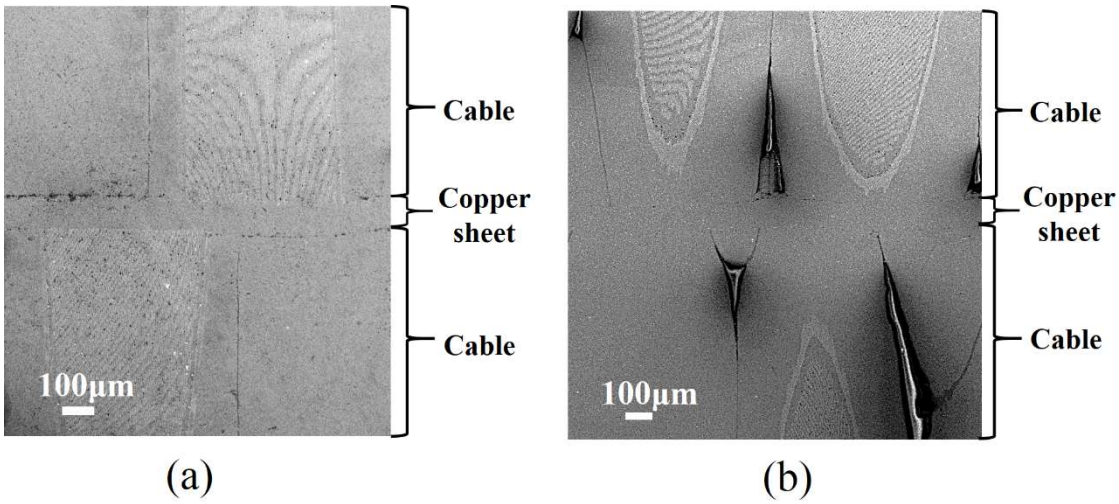

Fig. 8　Microstructure observation results of the butt joint interface at a strand scale. (a) Filaments of Nb_3Sn strands are attached to the copper sheet.
(b) Cu stabilizer of Nb_3Sn strands are attached to the copper sheet.

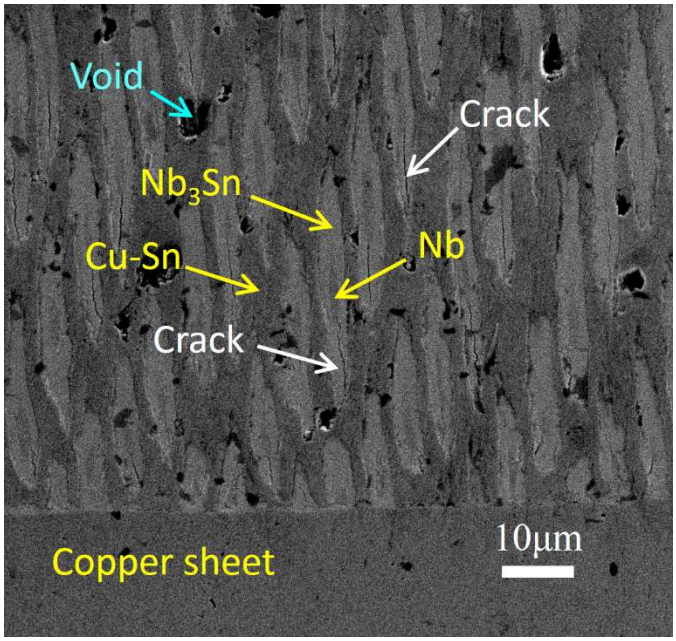

Fig. 9　Microstructure observation result of the butt joint interface at a filament scale.

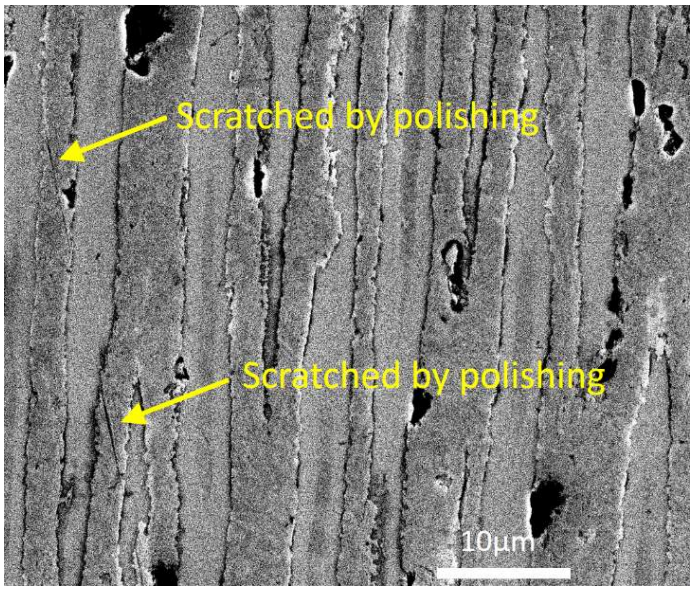

Fig. 10　Microstructure observation result of scratches by polishing.

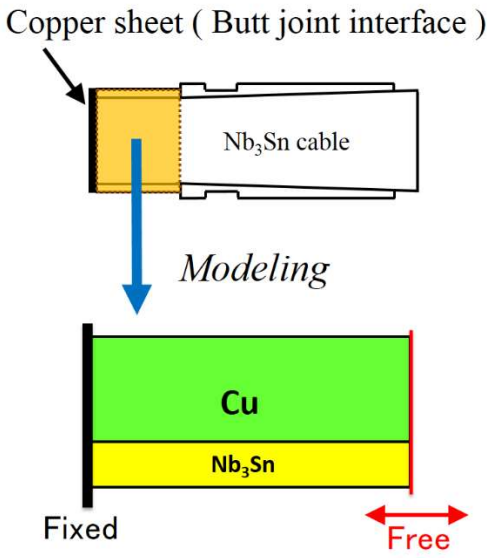

Fig. 11 Analytical model of the butt joint based on the theory of composites.